The EMBO Journal (2009) 28, 123–134 | © 2009 European Molecular Biology Organization | All Rights Reserved 0261-4189/09
www.embojournal.org

THE EMBO JOURNAL

Circadian gene expression is resilient to large fluctuations in overall transcription rates

Charna Dibner[1], Daniel Sage[2], Michael Unser[2], Christoph Bauer[3], Thomas d'Eysmond[4,5], Felix Naef[4,5] and Ueli Schibler[1,*]

[1]Department of Molecular Biology & NCCR Frontiers in Genetics, University of Geneva, Geneva, Switzerland, [2]Biomedical Imaging Group, Ecole Polytechnique Fédérale de Lausanne (EPFL), Lausanne, Switzerland, [3]NCCR Frontiers in Genetics, Imaging Platform, University of Geneva, Geneva, Switzerland, [4]Computational Systems Biology Group, Ecole Polytechnique Fédérale de Lausanne (EPFL), Lausanne, Switzerland and [5]Swiss Institute of Bioinformatics (SIB), Lausanne, Switzerland

Mammalian circadian oscillators are considered to rely on transcription/translation feedback loops in clock gene expression. The major and essential loop involves the autorepression of cryptochrome (*Cry1*, *Cry2*) and period (*Per1*, *Per2*) genes. The rhythm-generating circuitry is functional in most cell types, including cultured fibroblasts. Using this system, we show that significant reduction in RNA polymerase II-dependent transcription did not abolish circadian oscillations, but surprisingly accelerated them. A similar period shortening was observed at reduced incubation temperatures in wild-type mouse fibroblasts, but not in cells lacking *Per1*. Our data suggest that mammalian circadian oscillators are resilient to large fluctuations in general transcription rates and temperature, and that PER1 has an important function in transcription and temperature compensation.

The EMBO Journal (2009) **28,** 123–134. doi:10.1038/emboj.2008.262; Published online 11 December 2008
Subject Categories: chromatin & transcription; genomic & computational biology
Keywords: circadian clocks; fibroblasts; transcription compensation

Introduction

The mammalian circadian timing system has a hierarchical structure, in that a master pacemaker residing in the suprachiasmatic nucleus synchronizes slave oscillators existing in most body cells (Takahashi, 2004; Reppert, 2006). Cell-autonomous and self-sustained clocks were also found in cultured cells (Balsalobre *et al*, 1998; Nagoshi *et al*, 2004; Liu *et al*, 2007).

In 1990, Rosbash and co-workers (Hardin *et al*, 1990) discovered that the Drosophila clock protein Period (PER) inhibits the transcription of its own gene, and hence proposed a negative transcription/translation feedback loop as the operational principle for rhythm generation. Since then a large number of circadian clock genes have been identified in a variety of organisms from cyanobacteria to humans, and negative feedback loops are still the prevalent model for most of these organisms (Lakin-Thomas, 2006; Gallego and Virshup, 2007). In mammals, the CLOCK and BMAL1 transcription factors activate the expression of *Per* and *Cry* genes. Once PER and CRY concentrations have reached a critical threshold, they attenuate the CLOCK/BMAL1-mediated activation of their own genes in a negative feedback loop (Hastings and Herzog, 2004; Reppert, 2006). However, posttranslational events, such as the control of protein phosphorylation, acetylation, degradation, sumoylation and nucleocytoplasmic shuttling, contribute critically to the circadian rhythm generation and may affect period length, amplitude and/or magnitude of the oscillations (Lee *et al*, 2001; Cardone *et al*, 2005; Asher *et al*, 2008).

Although most physiological processes run faster at higher temperature, the period length of circadian oscillators remains nearly constant over a wide range of physiological temperatures (Konopka *et al*, 1989; Kaushik *et al*, 2007; Takeuchi *et al*, 2007). This even applies to circadian oscillators of homoeotherm organisms, such as those operative in cultured mammalian fibroblasts (Izumo *et al*, 2003; Tsuchiya *et al*, 2003). Here, we show that circadian clocks of fibroblasts are also compensated for global transcription rates. Considering that intrinsic transcription rates vary significantly in cells from different tissues (Schmidt and Schibler, 1995), transcription compensation may be an important property of peripheral circadian clocks.

Results

Long-term inhibition of RNA polymerase II-dependent transcription

Global transcription rates can be attenuated by the exposure of cells to various drugs that function at different steps. The most widely used compounds are actinomycin D and α-amanitin. Actinomycin D intercalates into double-stranded DNA and blocks transcription elongation by all three polymerases, RNA polymerase I (Pol I) being particularly sensitive. α-Amanitin is a selective and specific inhibitor of RNA polymerase II (Pol II) and RNA polymerase III (Pol III) *in vitro* and *in vivo*, with Pol II being considerably more sensitive than Pol III. α-Amanitin binds to RPB1, the largest Pol II subunit, with high affinity and thereby prevents translocation by blocking Pol II bridge helix bending (Bushnell *et al*, 2002). In addition, this drug induces the ubiquitination of the C-terminal domain of RPB1 and elicits proteasome-mediated RPB1 degradation in a dose-dependent manner (Nguyen *et al*, 1996; Mitsui and Sharp, 1999; Arima *et al*, 2005).

To examine the impact of overall transcription rates on circadian oscillator function, we analysed circadian gene expression in α-amanitin- and actinomycin D-treated

*Corresponding author. Department of Molecular Biology & NCCR Frontiers in Genetics, University of Geneva, Sciences III, 30, Quai Ernest Ansermet, Geneva 1211, Switzerland. Tel.: +41 22 379 6175; Fax: +41 22 379 6868; E-mail: ueli.schibler@unige.ch

Received: 24 July 2008; accepted: 24 November 2008; published online: 11 December 2008

fibroblasts. To this end, we had to identify conditions that allowed the recording of gene expression for extended time periods. Long-term treatment with α-amanitin and actinomycin D at concentrations higher than 0.5 μg/ml and 10 nM, respectively, caused significant cell death (Supplementary Figure 1A and B). However, the pretreatment of cells with sublethal doses of α-amanitin and actinomycin D for 16 and 5 h, respectively, allowed the recording of circadian bioluminescence during at least 3 days at reduced transcription rates (see Figure 1A for experimental design).

To validate this approach, we estimated the inhibitory effects of α-amanitin and actinomycin D on Pol II-dependent transcription by several methods (Figure 1B–E) and assayed transcription rates or RPB1 expression during 48–72 h after the drugs were washed away. First, *in vivo* transcription rates in NIH3T3 cells pretreated for 16 h with α-amanitin (3–5 μg/ml) or in untreated cells were measured by the incorporation of [^{3}H]uridine after labelling the cells for 60 min (Figure 1B). In keeping with previous publications (Adolph *et al*, 1993), we found that pretreatment of NIH3T3 cells with 3 and 5 μg/ml of α-amanitin for 16 h reduced RNA synthesis to about 60 and 35%, respectively, when compared with untreated cells (Figure 1B, panel 0 h). The inhibitory effect of α-amanitin on overall transcription rates persisted for at least 48 h (Figure 1B). In the second approach, *in vitro* incorporation of [^{32}P]UTP (uridine triphosphate) was measured in isolated cell nuclei by run-on transcription assays under conditions favouring efficient elongation

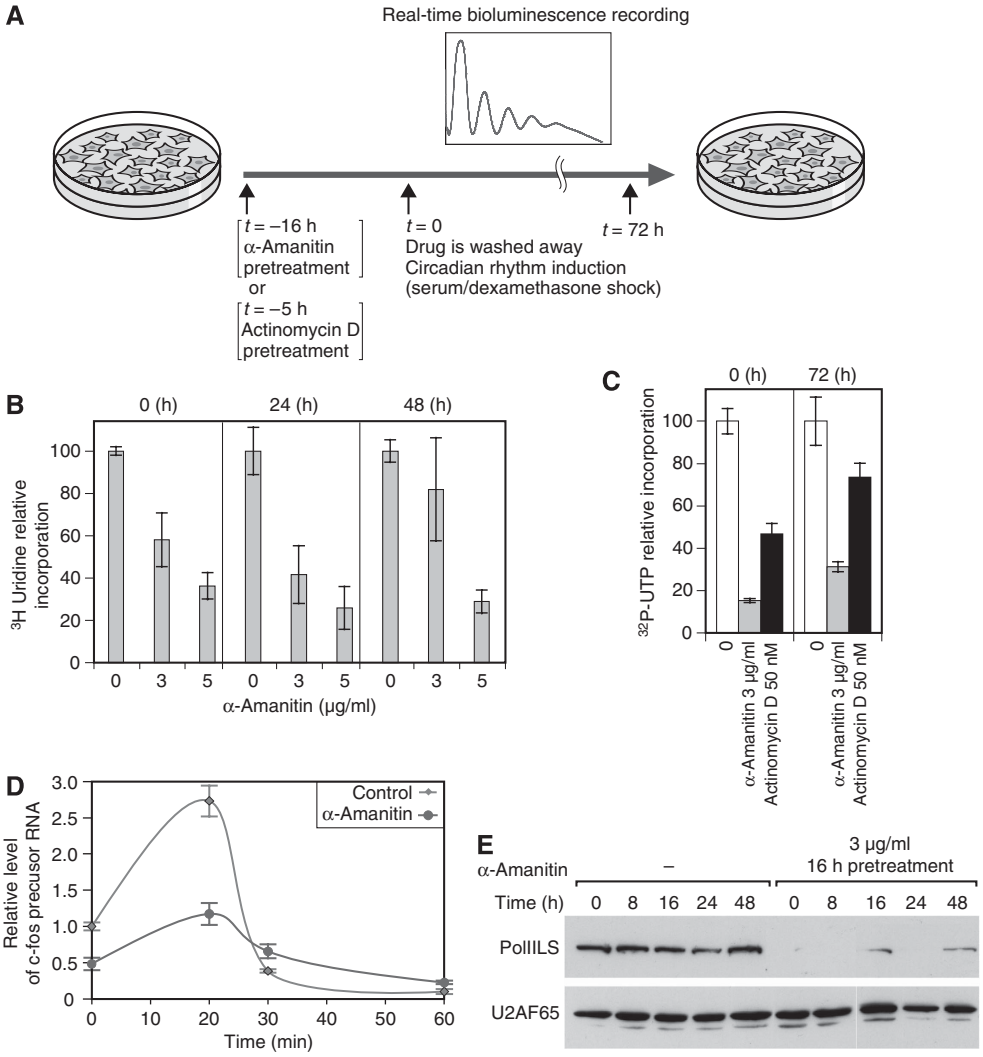

Figure 1 Reduction of RNA polymerase II-mediated transcription by sublethal concentrations of α-amanitin and actinomycin D. (**A**) Experimental design scheme. (**B**) [^{14}C]Thymidine-prelabeled NIH3T3 cells were treated for 16 h with 0–5 μg/ml of α-amanitin and pulse-labeled with [^{3}H]uridine for 60 min at the indicated time points. Transcription rates were calculated on a per DNA basis as described in Materials and methods. Pretreatment of NIH3T3 cells with 3 μg/ml of α-amanitin for 16 h reduced RNA synthesis to 58 ± 13% relative to untreated control ($n = 5$); with 5 μg/ml of α-amanitin to 36 ± 6% ($n = 4$; panel 0 h). At 24 h after α-amanitin removal, the relative transcription rates amounted to 42 ± 14% ($n = 5$) and 26 ± 6% ($n = 4$), respectively, for the two drug concentrations (panel 24 h), and 48 h after drug removal, they amounted to 81 ± 24% ($n = 5$) and 29 ± 5% ($n = 4$; panel 48 h), respectively. (**C**) Relative run-on transcription rates were determined for nuclei of NIH3T3 fibroblasts pretreated with 3 μg/ml of α-amanitin for 16 h or with 50 nM actinomycin D for 5 h. (**D**) Expression profiles of *c-fos* precursor RNA from untreated cells and cells pretreated with 3 μg/ml α-amanitin during 16 h. Cells were collected at the indicated time points after horse serum addition (time 0); transcripts were quantified as described in Materials and methods. (**E**) Western blot analysis of whole-cell extracts from untreated cells and cells pretreated with 3 μg/ml α-amanitin. The antibodies used recognize the RPB1 and the splicing factor U2AF65 (loading control).

predominantly by Pol II (Gariglio *et al*, 1981; Schmidt and Schibler, 1995). Pretreatment with α-amanitin (3 μg/ml) abolished about 85% of Pol II-dependent transcription immediately after drug elimination, and about 70% after 72 h (Figure 1C). Actinomycin D (50 nM) inhibited about half of Pol II-dependent transcription immediately after drug removal, with partial recovery to 73% after 72 h (Figure 1C). We noticed that the incorporation rate of uridine into RNA in α-amanitin-pretreated cells (Figure 1 B) was somewhat higher after 48 h than expected on the basis of the *in vitro* run-on experiments performed with cells analysed 72 h after the pretreatment (Figure 1C). This may have been caused by a reduction of the nuclear UTP pool size, which is difficult to measure experimentally.

Next, we determined the effect of α-amanitin on the induction of *c-fos* precursor RNA by a serum shock (Adolph *et al*, 1993) and found that this immediate early response was significantly dampened in drug-treated cells (Figure 1D). Finally, we evaluated α-amanitin-mediated RPB1 degradation. As shown in Figure 1E, a western blot analysis revealed a strong reduction in RPB1 protein levels after a 16-h treatment of cells with 3 μg/ml α-amanitin, and RPB1 accumulation remained low for at least 48 h (Figure 1E).

Inhibition of clock gene transcription by α-amanitin

To determine the impact of α-amanitin treatment on the transcription of core clock genes, mRNA accumulation patterns for synchronized NIH3T3 cells were monitored by quantitative RT–PCR using amplicons for *Bmal1*, *Rev-erbα*, *Dbp*, *Per1* and *Per2*. The values thus obtained were then normalized to Q-PCR values measured for a *Gapdh* amplicon in genomic DNA from duplicate plates, to express transcript accumulation levels in cellular equivalents (see Materials and methods). As shown in Figure 2, the α-amanitin treatment inhibited the cellular accumulation of transcripts specified by all examined core clock and clock-controlled genes, albeit to somewhat different extents. Genes such as *Per1*, *Per2* and *Dbp*, the transcription of which is activated by BMAL1-CLOCK and repressed by PER–CRY complexes, were particularly sensitive to α-amanitin treatment. In addition, the serum-induced immediate early induction of *Per1* and *Per2* expression was strongly blunted in drug-treated cells (Figure 2). Although these experiments suggested that NIH3T3 clocks still function in α-amanitin-treated cells, the low magnitude, amplitude and temporal resolution observed in the temporal mRNA accumulation profiles did not allow for a more detailed characterization of circadian phenotypes caused by the reduction of global transcription rates. Hence, we resorted to more sensitive reporter gene assays with a high temporal resolution power.

Circadian gene expression is resilient to large fluctuations in transcription rates

Fibroblasts expressing fire fly luciferase from circadian promoters exhibit robust circadian bioluminescence rhythms in synchronized cell populations and individual cells (Nagoshi *et al*, 2004; Liu *et al*, 2007). To assess the impact of reduced transcription on circadian gene expression, we monitored

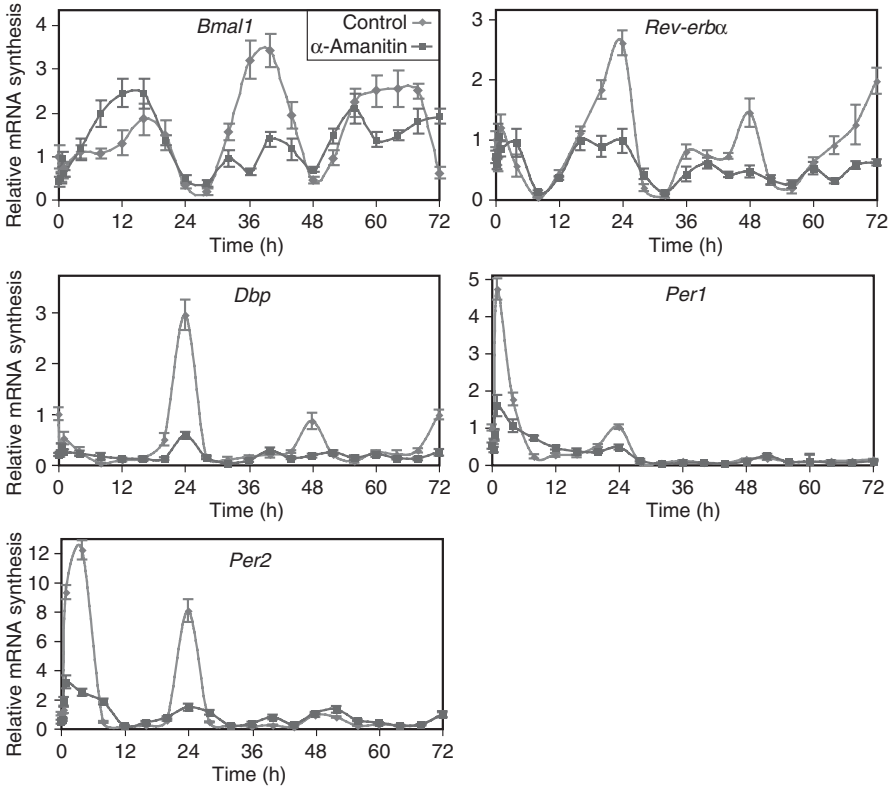

Figure 2 Endogenous core clock genes oscillate with a lower circadian amplitude at reduced Pol II-dependent transcription rates. Expression profiles of *Bmal1*, *Rev-erbα*, *Dbp*, *Per1* and *Per2* mRNA from untreated cells and cells pretreated with 3 μg/ml α-amanitin for 16 h. The cells were collected at the indicated time points after the addition of horse serum (time 0). The relative mRNA levels were determined by qRT–PCR analysis and normalized to genomic DNA (see Materials and methods).

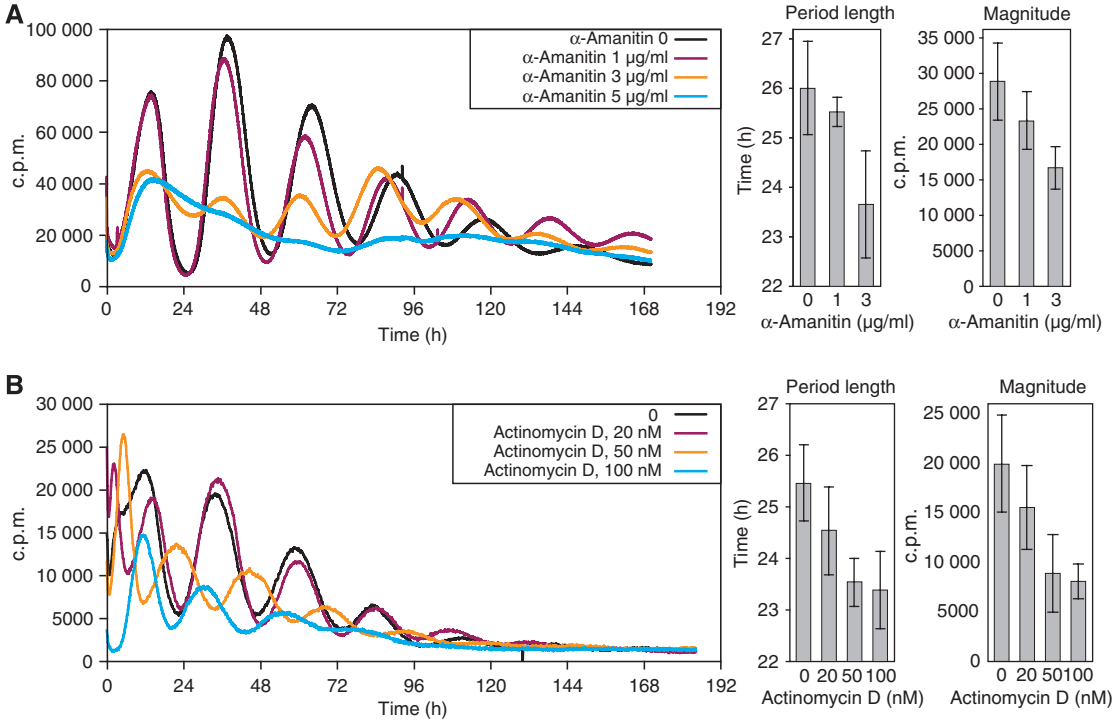

Figure 3 NIH3T3 circadian oscillators are functional at significantly reduced RNA polymerase II-dependent transcription rates. (**A**) NIH3T3 Bmal1-luc cells (grown to confluence) were incubated for 16 h in the presence of 0–5 μg/ml of α-amanitin. At time 0, cells were induced by dexamethasone, α-amanitin was removed and bioluminescence was recorded for 172 consecutive hours (left panel). Increasing doses of α-amanitin resulted in progressively shorter period lengths. The mean period lengths ± s.d. determined in '*n*' repetitions in five independent experiments were 25.9 ± 0.9, 25.5 ± 0.3 and 23.6 ± 1.1 h for 0, 1 and 3 μg/ml of α-amanitin, respectively; $n = 18$; see middle panel. The magnitudes (maximal photon counts) decreased with increasing α-amanitin concentrations (right panel). Using bilateral *t*-test for statistical analysis, the following significance values were obtained for data sets from cells on 3 μg/ml of α-amanitin treatment compared with untreated samples: for period length change $P = 7 \times 10^{-5}$; for magnitude $P = 0.01$. (**B**) NIH3T3 Bmal1-luc cells were incubated for 5 h in the presence of 0–100 nM of actinomycin D. At time 0, cells were treated with dexamethasone, actinomycin D was washed away and bioluminescence was recorded for 186 h (left panel). Increasing doses of actinomycin D resulted in progressively shorter period length: 25.4 ± 0.7, 24.5 ± 0.9, 23.5 ± 0.5 and 23.3 ± 0.7 h for 0, 20, 50 and 100 nM of actinomycin D, respectively; $n = 5$; see middle panel. The magnitudes were reduced by the drug treatment (right panel). The following significance values were obtained for data sets from cells on 50 nM of actinomycin D treatment compared with control: $P = 0.001$; for magnitude $P = 0.018$.

circadian bioluminescence of synchronized NIH3T3 fibroblasts stably expressing luciferase driven from *Bmal1* promoter (Nagoshi *et al*, 2004) after a 16-h pretreatment with sublethal concentrations of α-amanitin and actinomycin D. As shown in Figure 3A, robust bioluminescence cycles could be detected in cells pretreated with 1–3 μg/ml of α-amanitin, and residual oscillation was observed in experiments with 5 μg/ml. As expected, the magnitude of Bmal1-luc expression progressively decreased with increasing α-amanitin concentrations (Figure 3A, right panel). Unexpectedly, however, period length gradually shortened with decreasing overall transcription rates (Figure 3A, middle panel). Thus, cells pretreated with 3 μg/ml α-amanitin oscillated with a 2.3-h shorter period than untreated cells. Actinomycin D pretreatment had similar effects on the bioluminescence cycles generated by Bmal1-luc cells (Figure 3B, left panel). Similar to α-amanitin, actinomycin D reduced the magnitude, amplitude and period length of circadian Bmal1-luc expression (Figure 3B). Pretreatment with α-amanitin and actinomycin D also caused a shortening of the period length and a dampening of amplitude and magnitude of bioluminescence cycles produced by skin tail fibroblasts from *mPer2::luciferase* mice (Supplementary Figure 2A and B). α-Amanitin had a similar effect on NIH3T3 cells expressing luciferase from *Dbp* regulatory sequence oscillation pattern (Supplementary Figure 2C).

As shown in Supplementary Figure 3, α-amanitin affected circadian gene expression to a similar extent in cells synchronized by a short incubation with dexamethasone, horse serum or glucose (Balsalobre *et al*, 2000; Hirota *et al*, 2002). Thus, the alterations in circadian gene expression caused by transcription-inhibiting drugs depend neither on the signalling pathways used for the synchronization of cells nor on the expressed circadian reporter genes.

Individual fibroblast clocks exhibit robust oscillations in cells with reduced global transcription rates

At the population level, Bmal1-1uc cells exhibited progressively lower amplitude and magnitude oscillations as transcription rates dropped (Figure 3). The reduction in amplitude could have reflected a dampening of individual oscillators, and/or an inefficient synchronization between oscillators. To discriminate between these possibilities, we analysed temporal Bmal1-luc expression in individual cells treated with or without 3 or 5 μg/ml of α-amanitin, using the Olympus LV 200 bioluminescence workstation, a highly sensitive photon-counting microscope (see Materials and methods). As demonstrated by the time-lapse video recording provided in Supplementary data and at representative single-cell bioluminescence profiles (Figure 4A, B (control panel) and E), most of the recorded untreated cells (90%) exhibited

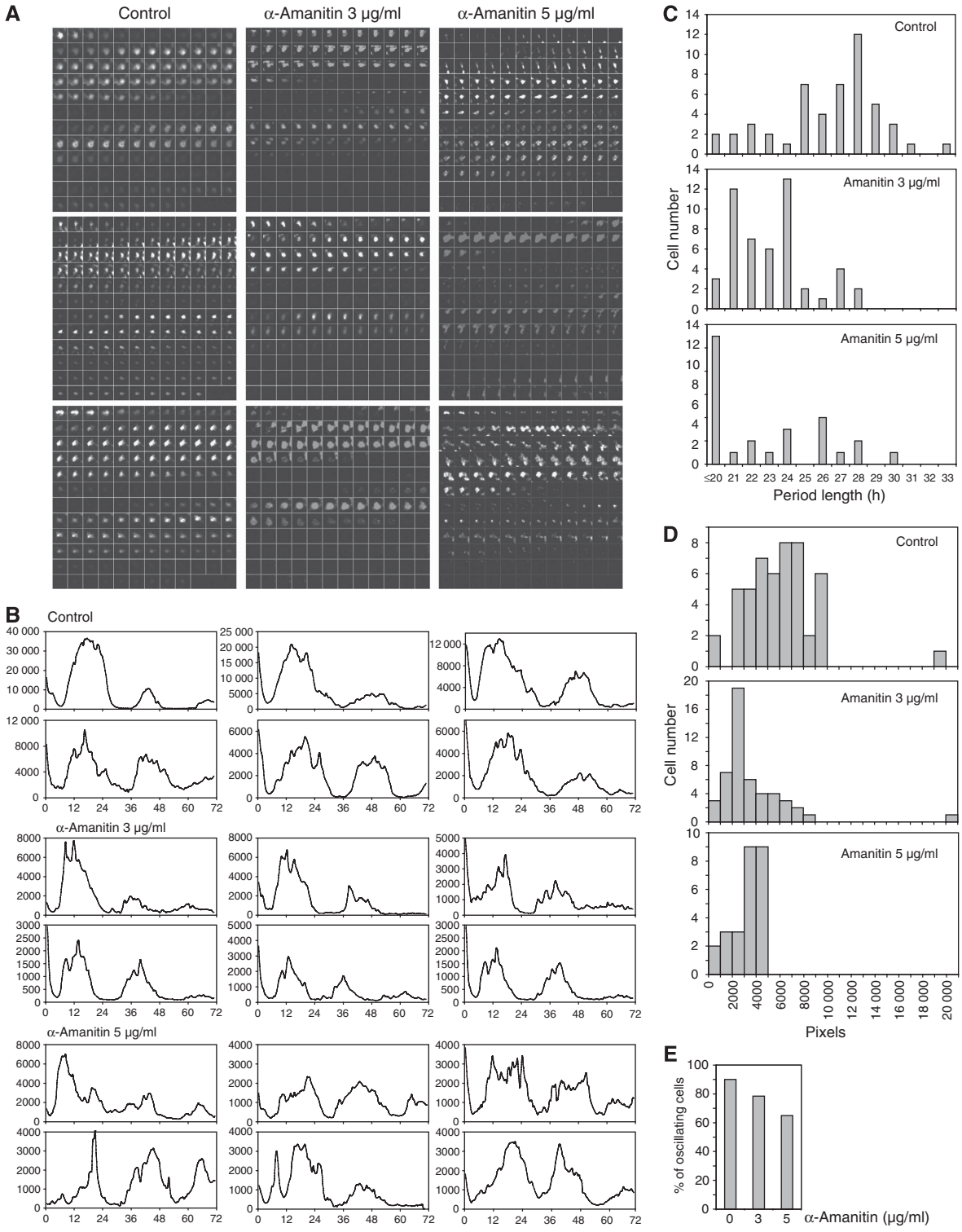

Figure 4 Individual α-amanitin-treated fibroblasts contain functional oscillators and have shorter period length. NIH3T3 Bmal1-luc fibroblasts (grown to confluence) were incubated for 16 h with DMEM + 10% FCS containing 0, 3 or 5 μg/ml of α-amanitin. At time 0, cells were synchronized by dexamethasone and time-lapse photon-counting microscopy was performed for three consecutive days as described in Materials and methods (see Supplementary movies 1–3, respectively). (**A**) Time-lapse microscopy of circadian Bmal1-luc expression in three individual cells each for untreated cells and cells pretreated with 3 or 5 μg/ml of α-amanitin. (**B**) Bioluminescence intensity profiles of six representative cells for each condition after synchronization with dexamethasone. (**C**) Histogram of period length distribution from 50 cells (control or 3 μg/ml α-amanitin) and 26 cells for 5 μg/ml α-amanitin. Period length was obtained from the best fit function as described in Supplementary data. The mean period lengths were 26.8 ± 2.7, 24.1 ± 3.6 and 23.4 ± 3.2 h, respectively, for 0, 3 and 5 μg/ml α-amanitin. (**D**) The signal intensity distribution (integrated pixels over the second peak) was calculated using the best fit function for 50 cells (control or 3 μg/ml α-amanitin) and 26 cells for 5 μg/ml α-amanitin. Mean sum intensities were 78 834.2 ± 33 394, 41 347 ± 18 097 and 37 806 ± 10 130 pixels × h for 0, 3 and 5 μg/ml α-amanitin, respectively. ANOVA analysis of data sets presented in (C, D) against each other yielded the following values: $P = 2 \times 10^{-10}$ for the period length values; $P = 7 \times 10^{-7}$ for mean sum intensities. (**E**) Percentages of oscillating cells among untreated cells ($N = 60$), cells pretreated with 3 μg/ml of α-amanitin ($N = 65$) and 5 μg/ml of α-amanitin ($N = 40$).

robust circadian oscillations. Here, 78% of cells pretreated with 3 μg/ml of α-amanitin also displayed rhythmic Bmal1-luc expression, albeit with a 25% lower magnitude on average, in comparison to untreated counterparts (Figure 4B (α-amanitin 3 μg/ml panel) and 4E; Supplementary data). Here, 65% of cells pretreated with 5 μg/ml of α-amanitin still exhibited circadian Bmal1-luc luminescence cycles, with 50% lower magnitude in comparison to control (Figure 4B (α-amanitin 5 μg/ml panel) and 4E; Supplementary data). For both period length and signal sum intensity, the distribution was clearly shifted towards lower values for α-amanitin-treated cells versus untreated control cells, and the mean values were in good agreement with our results obtained with cell populations (Figure 4C and D).

In conclusion, our single-cell recordings suggested that the partial inhibition of transcription by α-amanitin did not arrest cell-autonomous clocks, but rather dampened the magnitude and shortened the period length. In addition, α-amanitin treatment led to a wider distribution of period lengths. The blunted amplitudes of α-amanitin-treated cells revealed by population analysis were thus caused by smaller fraction of rhythmic cells, a widened period length distribution and reduced amplitude of individual cells.

Temperature and transcription compensation: manifestations of the same underlying principle?

Circadian oscillators have long been known to be temperature-compensated for both poikilotherm and homoeotherm organisms (Pittendrigh, 1954; Konopka *et al*, 1989). In fact, those of mammalian fibroblasts exhibit even a temperature 'overcompensation', that is, they run faster at lower temperatures (Izumo *et al*, 2003; Tsuchiya *et al*, 2003). In agreement with the conclusions made by these authors, our bioluminescence recordings obtained with Bmal1-luc cells (Figure 5A) and primary skin tail fibroblasts from *mPer2*::*luc* mice (Figure 6D) suggested a decrease in period length with descending temperature. As reduced temperature and transcription had similar effects on oscillator period length, we examined whether the period shortening is additive in α-amanitin-treated cells at reduced temperature. At 37°C, the drug affected circadian amplitude and period length as expected (Figure 5B). However, as depicted in Figure 5C, transcription inhibition had only a small effect on period length in cells incubated at 33°C. Hence, transcription and temperature compensation might be manifestations of similar oscillator features (see Discussion).

Temperature and transcription compensation in mPer1 knockout cells

As described earlier, the *per* gene has a key function in temperature compensation in *Drosophila*, and a mutation in the dimerization domain (PAS) of *per* renders the *Drosophila* oscillator temperature sensitive (Konopka *et al*, 1989). We thus wished to examine the possible role of Per1 in temperature and transcription compensation. As Per2-deficient fibroblasts are arrhythmic at the population level (Brown *et al*, 2005) and displayed unstable rhythms of low amplitude or were arrhythmic at the single-cell level (Liu *et al*, 2007), the role of PER2 in these processes could not be assessed. *Per1* knockout mice (Zheng *et al*, 2001) were crossed with *Per2*::*luc* knock-in reporter mice (Yoo *et al*, 2004). *Per1* knockout primary fibroblasts were shown to exhibit about

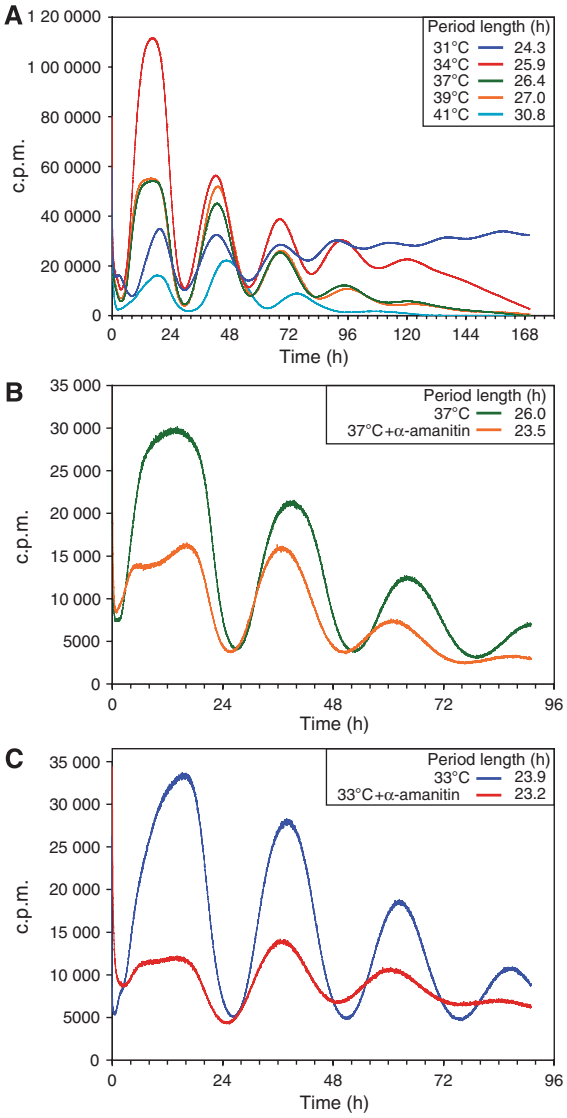

Figure 5 Transcription rates have mild effects on period length at reduced temperatures. (**A**) Bmal1-luc fibroblasts were synchronized with dexamethasone, placed into home-made precision incubators at temperatures ranging from 31 to 41°C, and bioluminescence cycles were recorded during 168 h. Of note, the period length progressively increases with elevated temperature. (**B**, **C**) Bioluminescence cycles from untreated and α-amanitin-treated (3 μg/ml) Bmal1-luc fibroblasts were recorded for 92 h at 33 or at 37°C. At 33°C, the α-amanitin-induced period shortening was less significant (23.21 ± 0.42 versus 23.96 ± 0.54 h) than at 37°C (23.52 ± 0.82 versus 26.03 ± 0.54 h). The following *P*-values were obtained for data sets compared with each other: period length from cells on 3 μg/ml of α-amanitin treatment compared with untreated samples at 37°C (B) $P = 0.001$ and at 33°C (C) $P = 0.12$.

3 h shorter circadian period in comparison to wild-type cells (Pando *et al*, 2002; Brown *et al*, 2005). In keeping with these observations, bioluminescence cycles produced by *Per1KO/Per2*::*luc* fibroblasts displayed 2–3 h shorter period as compared with their *Per1*$^{+/+}$/*Per2*::*luc* counterparts. Interestingly, however, the period length of these cells remained similar when transcription rates were reduced by a treatment with α-amanitin or actinomycin D (Figure 6A; period lengths for control, α-amanitin- and actinomycin D-treated cell lines are indicated on the graph). These values were similar when extracted from the mathematical

derivatives of the raw data curves, in which the oscillations are accentuated (Figure 6B). Unexpectedly, the amplitude—which was found to be low in untreated *Per1KO/Per2*::*luc* cells (Brown *et al*, 2005; Liu *et al*, 2007)—became somewhat more robust in actinomycin D-pretreated cells.

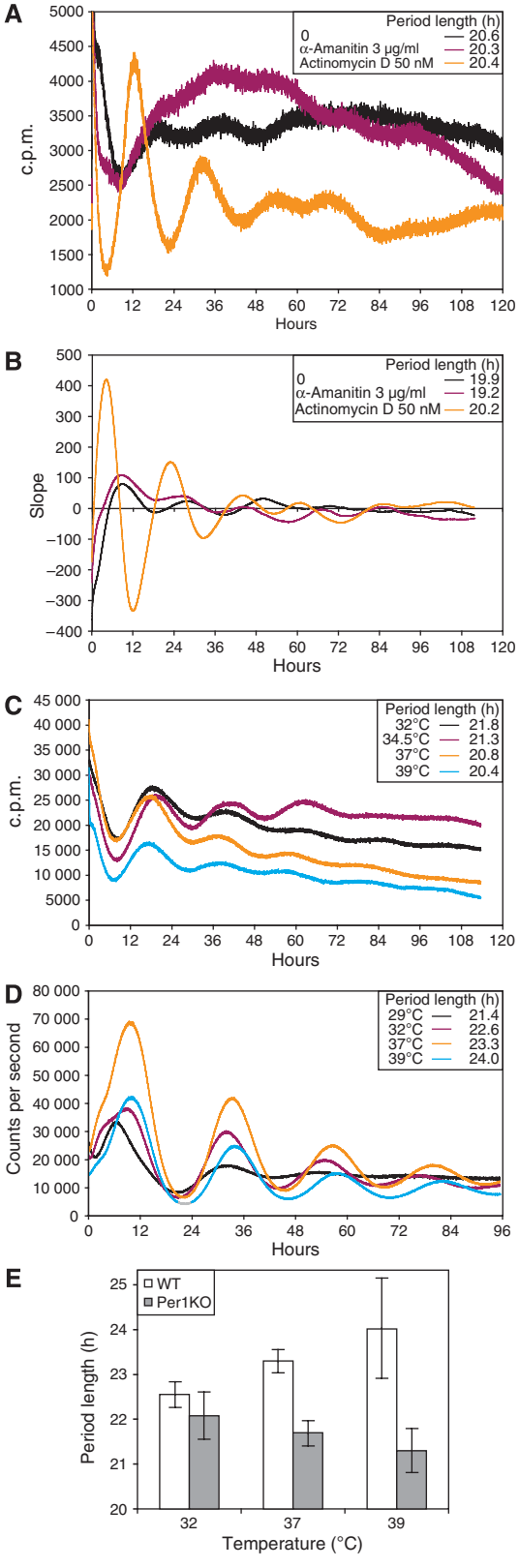

To characterize the oscillator properties of *Per1KO/Per2*::*luc* cells further, we assessed their bioluminescence cycles at different temperatures. Remarkably, the period length of these fibroblasts was about 1 hour shorter at higher temperature within the examined 32–39°C range (Figure 6C). Our analysis thus suggested that the period of *Per1KO* cells became slightly shorter at higher temperature, opposite from the trend observed for their wild-type counterparts (see Figure 6E for comparison of period length change as depicted in Figure 6C and D). Hence, the temperature 'overcompensation' typical for fibroblast oscillators depended on Per1, suggesting that this protein affects the mechanisms underlying both transcription and temperature compensation in mammalian cells.

Period and amplitude behaviour in common circadian oscillator models

To assess how our experimental findings compare with mathematical models for circadian oscillators, we simulated the period and the amplitude properties in two low-dimensional models (Figure 7A and B; Supplementary Figure 4A and B), and two higher dimensional kinetic models for the mammalian oscillator (Figure 7C and D; Supplementary Figure 4C and D). We hypothesized that transcription rates were reduced uniformly by the drugs and thus introduced the scale parameter ρ that rescales all mRNA synthesis rates. The low-dimensional models implement two prototypical designs for circadian oscillators, a delayed negative feedback loop (Figure 7A), related to the Goodwin oscillator (Gonze and Goldbeter, 2006), and a relaxation oscillator (Figure 7B) as proposed by Barkai and Leibler (2000). The first shows a period lengthening and amplitude increase with increasing transcription rates, consistent with our experimental finding (Figure 7A). A similar result was also found for another implementation of a Goodwin-type model (Kurosawa and Iwasa, 2005). In addition, the oscillatory regimen persists

Figure 6 Per1 influences the response of fibroblast oscillators to changes in global transcription rates and temperature. Skin tail primary fibroblasts from *Per1KO/Per2*::*luc* mice were pretreated for 16 h with 3 μg/ml α-amanitin, or for 5 h with 50 nM actinomycin D, and compared with untreated cells. Note that the mean period lengths determined in five independent experiments (indicated in the graph) did not change dramatically in response to these drugs, but that the amplitude increased in actinomycin D-treated cells. (**B**) Raw data from experiment (**A**) was subjected to linear regression analysis: slopes indicated at *Y* axes were calculated for 542 time points representing 9 h. (**C**) Bioluminescence cycles produced by *Per1KO/Per2*::*luc* mouse tail primary fibroblasts were recorded at different temperatures as described in the legend of Figure 5. The cells were oscillating with progressively shorter period at increasing temperatures. (**D**) *Per2*::*luc* mouse tail fibroblasts (immortalized with an expression vector encoding SV40 virus large T antigen) were grown to confluence, synchronized with dexamethasone, placed into individual boxes preheated to temperatures varying from 29 to 39°C, and bioluminescence was recorded for 168 h. Note that period length gets progressively longer with temperature increase. (**E**) Period length from Per1KO cells (C) and their wild-type counterparts (D) are plotted against temperature and have the opposite trends. The following *P*-values were obtained for data sets compared with each other: period length from Per1KO cells on 3 μg/ml of α-amanitin treatment compared with untreated Per1KO samples (A, B) $P=0.2$; for actinomycin D treatment $P=0.3$; for period length change at 32°C in comparison to 39°C for P1KO cells $P=0.1$ (C); for wt $P=0.03$ (D), with the opposite trend.

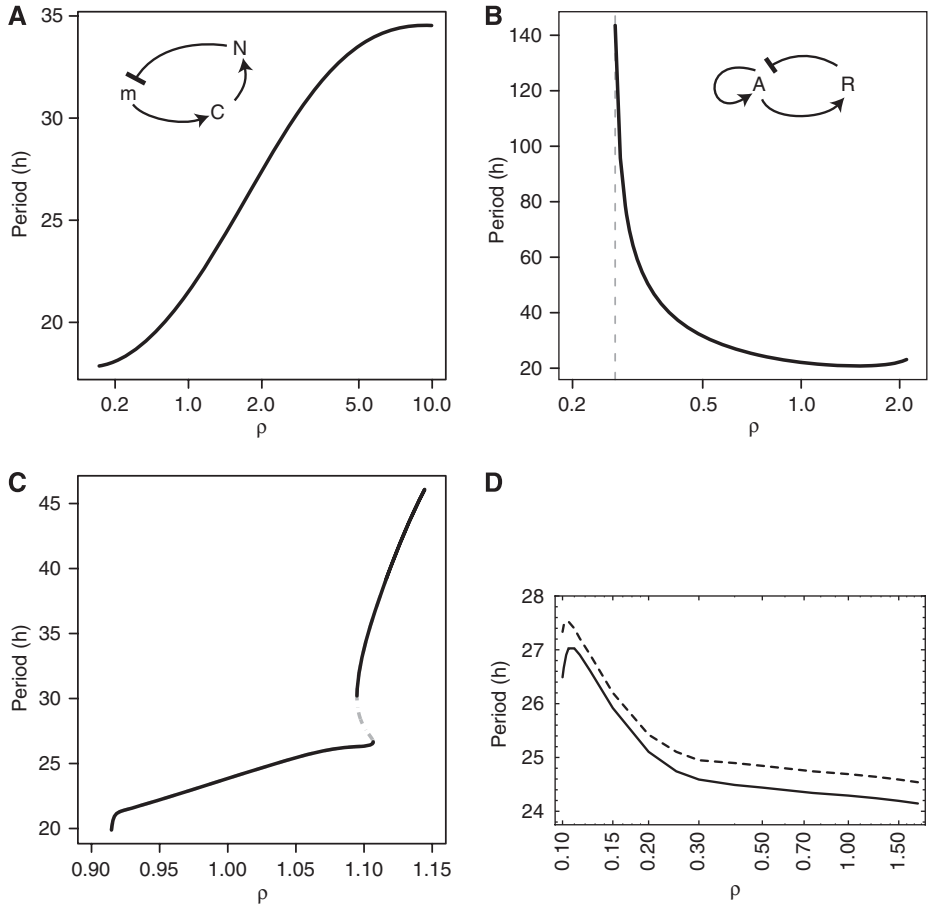

Figure 7 Period as a function of global transcription rates in common circadian oscillator models. The parameter ρ is a multiplicative factor that controls all transcription rates, ρ = 1 corresponds to the published nominal parameter values. Two simple low-dimensional models (**A**, **B**) and two more detailed models (**C**, **D**) are shown. (A) The *three species Gonze-Goldbeter delayed negative feedback model* with a messenger (m), a cytoplasmic (C) and nuclear repressor (N) shows onset of oscillation at ρ = 0.43 (Hopf bifurcation). Oscillations are kept when the transcription rate is raised by at least 20-fold. Period length initially rapidly increases with transcription, and then levels off at $T \sim 34$ h. The variation of the period with increased transcription ρ is positive around ρ = 1. The period lengthens with increasing ρ around ρ = 1. (B) A *minimal two species relaxation (hysteresis-based) oscillator* given by the equations for an activator (A) and a repressor (R):

$$\frac{dA}{dt} = s - d_A A + f\frac{A^2}{1+A^2} - eAR, \frac{dR}{dt} = kAR - d_R R$$

with parameters $s = 0.064$ [A]/h, $d_A = 0.32$/h, $f = 5.8$ [A]/h, $e = 1.6$ [R]$^{-1}$/h, $k = 0.64$ [A]$^{-1}$/h and $d_R = 0.15$/h. Here, transcription and translation processes are taken together. The model has an infinite period bifurcation near ρ = 0.27 and a Hopf bifurcation at ρ = 2.2. The period shortens with increasing ρ around ρ = 1. (C) The *16-dimensional mammalian model by Leloup and Goldbeter*. With its standard parameters, this model has a very narrow range of oscillation around ρ = 1 within ~10% of variation of the transcription rates in either direction (Hopf bif urcations at ρ = 0.94 and ρ = 1.14). Furthermore, the model shows a cyclic fold in a narrow window around ρ = 1.1 with coexistence of two stable (plain) and one unstable limit cycle (dashed line). The period lengthens with increasing ρ around ρ = 1. (D) *The 74-dimensional mammalian Forger–Peskin model*. Here, the model has both *Per1* and *Per2* genes, and it is thus also possible to simulate the *Per1* knockout phenotypes (dashed line). In contrast to the experimental data, the *Per1* mutant oscillators display slightly longer periods. Transcription can be reduced almost to zero while keeping oscillations. The period shortens with increasing ρ around ρ = 1. Oscillation amplitudes for the same four models are shown in Supplementary Figure 4.

for reduction in transcription as large as 40%. Our implementation of a relaxation oscillator shows a relatively stable period dependency in a range around ρ = 1, as expected for a relaxation oscillator (Barkai and Leibler, 2000). However, the period globally decreases with transcription rate (Figure 7B) and seems thus unable to account for the experimental data presented here. We now turn to more detailed mammalian models. Even though the Leloup–Goldbeter model (Leloup and Goldbeter, 2003) exhibits the right sign in the dependency of period length on transcription, the transcription range in which the model oscillates is much narrower than observed experimentally (Figure 7C); thus, this model and its parameters are in qualitative agreement with the data. Notice, however, that alternate parameter sets for the same model have been subsequently proposed (Leloup and Goldbeter, 2003), one of which exhibits a wider oscillatory range in the function of the transcription rate. Similar to the relaxation oscillator, the detailed Forger–Peskin model has an opposite period dependency (Forger and Peskin, 2003). Moreover, the half-hour period increase in the simulated case of *Per1* knockout is inconsistent with experiments performed by us and others (Zheng *et al*, 2001; Brown *et al*, 2005). These simulations thus indicate limited predictability by some of the commonly invoked kinetic models, and suggest that basic architectures based on the Goodwin model come closest to capturing qualitatively the period shortening observed on

reducing transcription rates. In fact, the Bmal1 loop in the Leloup–Goldbeter model is very much reminiscent of the three species Goodwin-type model.

Discussion

Fibroblast circadian oscillators are resilient to large reductions in transcription rates

We demonstrate here that circadian oscillators keep running in mouse fibroblasts in which overall Pol II-dependent transcription rates are reduced up to three-fold. Inhibition of transcription dampened the magnitudes and amplitudes of clock gene expression cycles but did not eliminate them. The observed resilience to reduced overall transcription rates cannot be readily explained by a compensation of core clock gene expression at the level of protein accumulation, as in α-amanitin-treated cells, decreased *Per2* and *Cry2* mRNA levels were accompanied by reduced PER2 and CRY2 protein levels (Supplementary Figure 5). Hence, the negative feedback loop does not appear to be based on a stoichiometric mechanism requiring absolute cellular threshold concentrations of CRYs and PERs. Rather, these proteins may function as cofactors in enzymatic processes, for example those involved in regulating the circadian DNA affinity of BMAL1 and/or CLOCK/NPAS2, critical activators of *Per* and *Cry* genes. BMAL1 and CLOCK and their *Drosophila* orthologues CLK and CYC accumulate at similar levels throughout the day, but display a rhythmic affinity for their E-box cognate sequences both *in vivo* and *in vitro* (Ripperger and Schibler, 2006; Reinke *et al*, 2008; Taylor and Hardin, 2008). In agreement with our statement of mammalian oscillator compensation for large changes in transcription, Fan *et al* (2007) have demonstrated that CRY1, CRY2 and BMAL1 protein oscillation were not necessary for proper oscillator function in mouse, Rat-1 and HEK293 cells. This report and our own findings are not supportive of the current version of canonical model of transcription–translation feedback loop.

In the circadian clock of the filamentous fungus *Neurospora crassa*, the repressor protein FRQ serves as a cofactor of protein kinases to modulate the cyclic DNA-binding activity of the transcription factor complex WCC (Brunner and Kaldi, 2008). A similar scenario may apply to the control of CLOCK and BMAL1 activity by PER and CRY proteins (Taylor and Hardin, 2008).

The circadian period shortening was observed irrespective of whether actinomycin D or α-amanitin was used to reduce overall transcription rates. We did observe, however, that actinomycin D also affected the phase and the sharpness of the first bioluminescence peak at the two lower concentrations (Figure 3B). At these doses, the drug is expected to completely suppress ribosomal Pol I-dependent transcription, whereas only partially inhibiting Pol II-mediated transcription. Conceivably, dexamethasone-induced immediate early expression (e.g. that of PER1)—which is responsible for the timing and duration of the first Bmal1-luc expression peak and the synchronization of cellular oscillators—is altered in cells with an increased mRNA/ribosome ratio. Alternatively, the arrest of ribosomal RNA transcription by RNA Pol I may release rate-limiting components required for immediate early gene expression. RNA Pol I accounts for a very large fraction of total nuclear RNA synthesis, and some regulatory proteins (e.g. TBP, TFIIH) are shared by the RNA Pol I and II transcription machineries (Eberhard *et al*, 1993; Iben *et al*, 2002).

The effect of reduced transcription rates on circadian gene expression was also examined by single-cell bioluminescence analysis (Supplementary movies 1–3). The period distribution of drug-treated cells was wider and shifted towards shorter values when compared with untreated cells. The broadening in period distributions is perfectly consistent with increased intrinsic noise resulting from a reduced number of transcripts (Gonze and Goldbeter, 2006). On average, the magnitudes of the bioluminescence cycles were reduced in drug-treated cells, as expected. In keeping with our circadian luciferase reporter data, the abundance of endogenous clock transcripts and proteins oscillated with a lower amplitude and magnitude under α-amanitin treatment. We noted, however, that reduced transcription affected the amplitude of *Bmal1* and *Rev-erbα* mRNA accumulation cycles somewhat less than that of *Per1*, *Per2* and *Dbp* accumulation cycles. Hence, the transcription control mechanisms of some clock genes might be somewhat more sensitive to this insult than those of others. Interestingly, a correlation between reduced amplitude and an increased sensitivity to phase-shifting stimuli was recently observed in primary fibroblasts from a large number of human subjects (Brown *et al*, 2008).

We also examined the effect of 5,6-dichloro-1-fl-D-ribobenzimidazole (DRB) on circadian gene expression. This drug inhibits transcription by preventing RPB1 phosphorylation and thereby the escape of Pol II from promoters (Dubois *et al*, 1994). In contrast to α-amanitin and actinomycin D, DRB actually lengthened the period by 3–3.5 h (data not shown). However, DRB is also a potent inhibitor of casein kinase 1δ/ε (CK1δ/ε) activity (Smith, 2002; Kim *et al*, 2008), and phosphorylation of circadian clock proteins by CK1δ/ε has a crucial but complex function in period length determination (Eide and Virshup, 2001; Lin *et al*, 2002). Although a mutation comprising PER2 phosphorylation and a hypomorphic mutation in CK1ε resulted in period shortening (Lowrey *et al*, 2000; Toh *et al*, 2001; Xu *et al*, 2005; Vanselow *et al*, 2006), the treatment of Rat-1 fibroblasts with the CKIδ/ε-selective inhibitor IC261 caused a period lengthening of circadian gene expression (Eide *et al*, 2005). Thus, we cannot formally exclude the possibility that the effects of actinomycin D or α-amanitin on period length is caused by protein stability changes or other, yet unknown post-translational mechanisms rather than by a general transcription reduction.

The notion that period length is determined by both transcription and post-translation regulatory mechanisms also emerged from studies on other systems. Kondo and coworkers demonstrated that in cyanobacteria circadian protein phosphorylation can persist in the absence of transcription and translation (Tomita *et al*, 2005) at some temperatures and even succeeded in reconstituting a circadian oscillator *in vitro* with only three clock proteins (KaiA, KaiB and KaiC) and ATP (Nakajima *et al*, 2005). However, the same group recently showed that *in vivo* circadian clock gene transcription is required for a fully operative clock, and that period length is determined by an interplay between KaiC phosphorylation and cyclic gene expression (Kitayama *et al*, 2008). Period length determination in the *Drosophila* circadian clock—which shares many components with the mammalian oscillator—also depends on an intricate cross-talk between transcription and post-translation events. Thus, loss of function

in DBT, the fruit fly homologue of CK1δ/ε, can either shorten or lengthen the period, depending on the precise location of the mutation (Muskus *et al*, 2007). Moreover, when the transcription transactivation potential of the CLK–CYC heterodimer is increased by fusing the strong acidic activation domain of the Herpes virus protein VP16 to CYC, the circadian period length considerably shortens (Kadener *et al*, 2008). However, So and Rosbash (1997) also reported on the importance of post-transcriptional regulation in shaping the temporal *per* mRNA accumulation curve. Conceivably, at reduced overall transcription rates this mechanism controlling circadian mRNA stability over-rides the effect of transcription strength. This mechanism is actually operative in flies carrying a gene lacking the normal promoter (transgene 7.2) instead of the wild-type *per* allele. In these flies, *per* transcription from spurious promoters is constitutively low, and cyclic mRNA accumulation is driven by post-transcriptional mechanisms. As circadian cell culture systems are not yet available for the fruit fly, the impact of lowering overall transcription rates on circadian gene expression could not yet be examined in this species.

PER1 is involved in both temperature and transcription compensation

In keeping with recently published reports (Izumo *et al*, 2003; Tsuchiya *et al*, 2003), our data demonstrate that circadian clocks of NIH3T3 mouse fibroblasts and primary mouse tail fibroblasts are compensated—or rather overcompensated—for temperature. In *Drosophila*, the Per protein has a key function in temperature compensation, and per^{L} mutant flies loose temperature compensation and exhibit longer periods at higher temperature (Konopka *et al*, 1989). Our results suggest that Per proteins also have an important function in the temperature control of circadian oscillators in mammalian cells. Thus, *Per1KO* primary mouse tail fibroblasts are not temperature-(over)compensated, and in contrast to their wild-type counterparts oscillate with similar or even slightly shorter periods at higher temperatures. Interestingly, the effects of reduced Pol II transcription rates and decreased temperature on period length shortening were not additive. Likewise, *Per1KO* fibroblasts, normally oscillating with a 20-h period, did not exhibit further period shortening upon reduced transcription. These results would be compatible with a model surmising that the same molecular mechanisms underlie transcription and temperature compensation, and that PER1 has a function in these mechanisms. It was suggested for *Drosophila* that temperature-sensitive PER protein homodimerization, phosphorylation, protein degradation or alternative splicing of pre-mRNAs might account for temperature compensation (Hong and Tyson, 1997; Leloup and Goldbeter, 1997). Moreover, the role of PER in temperature compensation seems to be tightly linked to CRY proper function (Kaushik *et al*, 2007). Similar mechanisms might be responsible for temperature compensation in mammals, and we are planning to address Per1 phosphorylation patterns and Per–CRY complex formation at different temperatures.

Unexpectedly, weak oscillation amplitudes in *Per1KO* mouse fibroblasts could be rendered more robust by an actinomycin D treatment, suggesting the need of an optimal balance between the levels of different clock components for circadian oscillator function. A similar conclusion has been reached in another study examining the cooperation between PER and CRY proteins (Oster *et al*, 2002). Unexpectedly, circadian rhythmicity and normal clock gene expression patterns were restored in *Per2* mutant mice by the inactivation of *Cry2* (but not *Cry1*).

The impact of global transcription rates on period length in mathematical models

Global changes in transcription and translation rates arise in the body from variations in nutrition, growth condition or temperature. The ability of circadian clocks to keep running accurately despite significant variation in transcription rates appears necessary for the oscillator to maintain synchrony under different physiological conditions. The influence of fluctuations on period length and period dispersion in simple and complex models for the mammalian clock emphasized the role of post-translational regulation on oscillator stability (Rougemont and Naef, 2007). Here, we showed how low-dimensional models for prototypical nonlinear oscillators based on delayed negative feedback or relaxation oscillators tolerate a large range in transcription rates for which self-sustained oscillations are maintained, similar to what we observed experimentally. Although both models show regimens in which the period is rather insensitive to transcription rates (Barkai and Leibler, 2000), their global period dependence on transcription shows opposite signs, with Goodwin-type models being in qualitative agreement with our experiments. The more detailed mammalian models studied here were only partially consistent with our data, suggesting that the complexity of mammalian circadian clockworks is not yet fully captured by commonly invoked models. Future analysis will clarify the generality of our conclusions. Taken together, our data are consistent with the scenario that both the elimination of *Per1* and the reduction of general transcription destabilize the limit cycles by bringing the system closer to the bifurcation boundaries. At the population level, low circadian amplitudes were observed in both cases, and additional single-cell analysis will thus further clarify the underlying mechanisms.

Materials and methods

RNA synthesis measurement by uridine pulse assay

Uridine pulse assay was performed as described by Balajee *et al* (1997). Briefly, NIH3T3 cells were pre-labeled with [^{14}C]thymidine, treated for 16 h with 0–5 μg/ml of α-amanitin and pulse-labeled with [^{3}H]uridine for 60 min at the indicated time points. Radioactivity incorporated into TCA-precipitated fraction was measured by scintillation counting. Transcription rates were calculated as the ratio of [^{3}H]uridine incorporation per unit time divided by [^{14}C]thymidine incorporation into each sample, corresponding to DNA content. Relative [^{3}H]uridine incorporation corresponds to the ratio of values obtained for untreated and drug-treated cells.

In vitro transcription run-on assay

Run-on transcription rates were determined in isolated nuclei under conditions favouring Pol II-dependent transcription (Gariglio *et al*, 1981; Schmidt and Schibler, 1995). *In vitro* transcription rates were calculated as [^{32}P]UTP incorporation per minute per 10^{6} cells. Relative incorporation corresponds to the ratio of values obtained for untreated and drug-treated cells.

RNA analysis by real-time quantitative PCR

Cells from triplicate plates were collected every 4 h by trypsinization, rinsed with PBS, divided into two halves from each plate and frozen at −70°C. Total RNA was prepared from half of each plate using Trizol reagent and used as a substrate for cDNA synthesis. Genomic DNA was prepared from the other half of each plate using

the NucleoSpin Tissue kit (Macherey–Nagel). RNA and genomic DNA quantification by TaqMan real-time PCR was performed as described by Heid *et al* (1996). Briefly, 1 μg of total RNA was reverse-transcribed using M-MLV Reverse Transcriptase (Invitrogen) and random hexamers. The resulting cDNA and genomic DNA were PCR-amplified in an ABI PRISM 7700 Sequence Detection System from PE-Applied Biosystems. Primers and probes are listed in Supplementary Table 1.

Western blot experiments

Western blot experiments with whole-cell extracts were performed with antibodies against RPB1 and U2AF65 (loading control).

Cell lines and constructs

NIH3T3 Bmal1-luc cells are described by Nagoshi *et al* (2004). Mouse primary skin fibroblasts were prepared from *mPer1*$^{-/-}$ *mPer2*::*luciferase* or from *mPer2*::*luciferase* tail tips by standard procedure and grown in DMEM with 20% FCS. Where indicated, cells were immortalized by transfection with Large T Antigen SV40 (pBABE-puro SV40LT; Addgene; plasmid number 13970) and selected over several weeks.

Real-time bioluminescence monitoring

Cells were stimulated with either 50% horse serum or 100 nM dexamethasone as described (Nagoshi *et al*, 2004). Cultures were maintained at 37°C in a light–tight incubator and bioluminescence was monitored continuously using Hamamatsu photomultiplier tube detector assemblies. Photon counts were integrated over 1-min intervals.

Bioluminescence time-lapse microscopy and data analysis

NIH3T3 Bmal1-luc cells were plated in 35-mm glass bottom dishes (WillCo-dish, type 3522; WillCo Wells BV). After treating the cells with dexamethasone during 15 min, the medium was replaced by 2 ml phenol red-free DMEM supplemented with 10% FCS and 1 mM luciferin. Bioluminescence imaging was performed on an Olympus LV 200 bioluminescence workstation equipped with a ×20 UPLSAPO objective (NA 0.75). Bioluminescence emission was detected for several consecutive days using an EM CCD camera (Image EM C9100-13; Hamamatsu, Japan) cooled to −90°C using exposure times of 30 min. The image series were analysed using the ImageJ 1.32 software (National Institutes of Health, Bethesda, MD, USA; as described in Supplementary data).

Supplementary data

Supplementary data are available at *The EMBO Journal* Online (http://www.embojournal.org).

Acknowledgements

We thank Juergen Ripperger and Urs Albrecht for *mPer1* knockout mice; Hans Reinke, Gad Asher, David Gatfield and Steven Brown for critical comments; Emi Nagoshi for cell lines, Jerome Bosset for microscopy help, Andre Liani for having constructed the temperature regulated lumicycler, and Nicolas Roggli for the artwork. This research was supported by the Swiss National Foundation (through individual research grants to US, FN, DS and MU), the National Center of Competence in Research Program Frontiers in Genetics, the University of Geneva, the Ecole Polytechnique Fédérale de Lausanne (EPFL), the Louis Jeantet Foundation of Medicine (US), the Bonizzi-Theler Stiftung (US), the 6th European Framework Project EUCLOCK (US), the Hasler Foundation (DS and MU), the Gebert-Rüf Foundation (DS and MU). CD received a postdoctoral fellowship from the Roche Research Foundation.

References

Adolph S, Brusselbach S, Muller R (1993) Inhibition of transcription blocks cell cycle progression of NIH3T3 fibroblasts specifically in G1. *J Cell Sci* **105** (Part 1)**:** 113–122

Arima Y, Nitta M, Kuninaka S, Zhang D, Fujiwara T, Taya Y, Nakao M, Saya H (2005) Transcriptional blockade induces p53-dependent apoptosis associated with translocation of p53 to mitochondria. *J Biol Chem* **280:** 19166–19176

Asher G, Gatfield D, Stratmann M, Reinke H, Dibner C, Kreppel F, Mostoslavsky R, Alt FW, Schibler U (2008) SIRT1 regulates circadian clock gene expression through PER2 deacetylation. *Cell* **134:** 317–328

Balajee AS, May A, Dianov GL, Friedberg EC, Bohr VA (1997) Reduced RNA polymerase II transcription in intact and permeabilized Cockayne syndrome group B cells. *Proc Natl Acad Sci USA* **94:** 4306–4311

Balsalobre A, Brown SA, Marcacci L, Tronche F, Kellendonk C, Reichardt HM, Schutz G, Schibler U (2000) Resetting of circadian time in peripheral tissues by glucocorticoid signaling. *Science* **289:** 2344–2347

Balsalobre A, Damiola F, Schibler U (1998) A serum shock induces circadian gene expression in mammalian tissue culture cells. *Cell* **93:** 929–937

Barkai N, Leibler S (2000) Circadian clocks limited by noise. *Nature* **403:** 267–268

Brown SA, Fleury-Olela F, Nagoshi E, Hauser C, Juge C, Meier CA, Chicheportiche R, Dayer JM, Albrecht U, Schibler U (2005) The period length of fibroblast circadian gene expression varies widely among human individuals. *PLoS Biol* **3:** e338

Brown SA, Kunz D, Dumas A, Westermark PO, Vanselow K, Tilmann-Wahnschaffe A, Herzel H, Kramer A (2008) Molecular insights into human daily behavior. *Proc Natl Acad Sci USA* **105:** 1602–1607

Brunner M, Kaldi K (2008) Interlocked feedback loops of the circadian clock of *Neurospora crassa*. *Mol Microbiol* **68:** 255–262

Bushnell DA, Cramer P, Kornberg RD (2002) Structural basis of transcription: alpha-amanitin-RNA polymerase II cocrystal at 2.8 Å resolution. *Proc Natl Acad Sci USA* **99:** 1218–1222

Cardone L, Hirayama J, Giordano F, Tamaru T, Palvimo JJ, Sassone-Corsi P (2005) Circadian clock control by SUMOylation of BMAL1. *Science* **309:** 1390–1394

Dubois MF, Nguyen VT, Bellier S, Bensaude O (1994) Inhibitors of transcription such as 5,6-dichloro-1-beta-D-ribofuranosylbenzimidazole and isoquinoline sulfonamide derivatives (H-8 and H-7) promote dephosphorylation of the carboxyl-terminal domain of RNA polymerase II largest subunit. *J Biol Chem* **269:** 13331–13336

Eberhard D, Tora L, Egly JM, Grummt I (1993) A TBP-containing multiprotein complex (TIF-IB) mediates transcription specificity of murine RNA polymerase I. *Nucleic Acids Res* **21:** 4180–4186

Eide EJ, Virshup DM (2001) Casein kinase I: another cog in the circadian clockworks. *Chronobiol Int* **18:** 389–398

Eide EJ, Woolf MF, Kang H, Woolf P, Hurst W, Camacho F, Vielhaber EL, Giovanni A, Virshup DM (2005) Control of mammalian circadian rhythm by CKIepsilon-regulated proteasome-mediated PER2 degradation. *Mol Cell Biol* **25:** 2795–2807

Fan Y, Hida A, Anderson DA, Izumo M, Johnson CH (2007) Cycling of CRYPTOCHROME proteins is not necessary for circadian-clock function in mammalian fibroblasts. *Curr Biol* **17:** 1091–1100

Forger DB, Peskin CS (2003) A detailed predictive model of the mammalian circadian clock. *Proc Natl Acad Sci USA* **100:** 14806–14811

Gallego M, Virshup DM (2007) Post-translational modifications regulate the ticking of the circadian clock. *Nat Rev Mol Cell Biol* **8:** 139–148

Gariglio P, Bellard M, Chambon P (1981) Clustering of RNA polymerase B molecules in the 5′ moiety of the adult beta-globin gene of hen erythrocytes. *Nucleic Acids Res* **9:** 2589–2598

Gonze D, Goldbeter A (2006) Circadian rhythms and molecular noise. *Chaos* **16:** 026110

Hardin PE, Hall JC, Rosbash M (1990) Feedback of the *Drosophila* period gene product on circadian cycling of its messenger RNA levels. *Nature* **343:** 536–540

Hastings MH, Herzog ED (2004) Clock genes, oscillators, and cellular networks in the suprachiasmatic nuclei. *J Biol Rhythms* **19:** 400–413

Heid CA, Stevens J, Livak KJ, Williams PM (1996) Real time quantitative PCR. *Genome Res* **6:** 986–994

Hirota T, Okano T, Kokame K, Shirotani-Ikejima H, Miyata T, Fukada Y (2002) Glucose down-regulates Per1 and Per2 mRNA

levels and induces circadian gene expression in cultured Rat-1 fibroblasts. *J Biol Chem* **277:** 44244–44251

Hong CI, Tyson JJ (1997) A proposal for temperature compensation of the circadian rhythm in *Drosophila* based on dimerization of the per protein. *Chronobiol Int* **14:** 521–529

Iben S, Tschochner H, Bier M, Hoogstraten D, Hozak P, Egly JM, Grummt I (2002) TFIIH plays an essential role in RNA polymerase I transcription. *Cell* **109:** 297–306

Izumo M, Johnson CH, Yamazaki S (2003) Circadian gene expression in mammalian fibroblasts revealed by real-time luminescence reporting: temperature compensation and damping. *Proc Natl Acad Sci USA* **100:** 16089–16094

Kadener S, Menet JS, Schoer R, Rosbash M (2008) Circadian transcription contributes to core period determination in *Drosophila*. *PLoS Biol* **6:** e119

Kaushik R, Nawathean P, Busza A, Murad A, Emery P, Rosbash M (2007) PER–TIM interactions with the photoreceptor cryptochrome mediate circadian temperature responses in *Drosophila*. *PLoS Biol* **5:** e146

Kim MK, Kang MR, Nam HW, Bae YS, Kim YS, Chung IK (2008) Regulation of telomeric-repeat binding factor 1 binding to telomeres by casein kinase 2-mediated phosphorylation. *J Biol Chem* **283:** 14144–14152

Kitayama Y, Nishiwaki T, Terauchi K, Kondo T (2008) Dual KaiC-based oscillations constitute the circadian system of cyanobacteria. *Genes Dev* **22:** 1513–1521

Konopka RJ, Pittendrigh C, Orr D (1989) Reciprocal behaviour associated with altered homeostasis and photosensitivity of *Drosophila* clock mutants. *J Neurogenet* **6:** 1–10

Kurosawa G, Iwasa Y (2005) Temperature compensation in circadian clock models. *J Theor Biol* **233:** 453–468

Lakin-Thomas PL (2006) Transcriptional feedback oscillators: maybe, maybe not. *J Biol Rhythms* **21:** 83–92

Lee C, Etchegaray JP, Cagampang FR, Loudon AS, Reppert SM (2001) Posttranslational mechanisms regulate the mammalian circadian clock. *Cell* **107:** 855–867

Leloup JC, Goldbeter A (1997) Temperature compensation of circadian rhythms: control of the period in a model for circadian oscillations of the per protein in *Drosophila*. *Chronobiol Int* **14:** 511–520

Leloup JC, Goldbeter A (2003) Toward a detailed computational model for the mammalian circadian clock. *Proc Natl Acad Sci USA* **100:** 7051–7056

Lin JM, Kilman VL, Keegan K, Paddock B, Emery-Le M, Rosbash M, Allada R (2002) A role for casein kinase 2alpha in the *Drosophila* circadian clock. *Nature* **420:** 816–820

Liu AC, Welsh DK, Ko CH, Tran HG, Zhang EE, Priest AA, Buhr ED, Singer O, Meeker K, Verma IM, Doyle III FJ, Takahashi JS, Kay SA (2007) Intercellular coupling confers robustness against mutations in the SCN circadian clock network. *Cell* **129:** 605–616

Lowrey PL, Shimomura K, Antoch MP, Yamazaki S, Zemenides PD, Ralph MR, Menaker M, Takahashi JS (2000) Positional syntenic cloning and functional characterization of the mammalian circadian mutation tau. *Science* **288:** 483–492

Mitsui A, Sharp PA (1999) Ubiquitination of RNA polymerase II large subunit signaled by phosphorylation of carboxyl-terminal domain. *Proc Natl Acad Sci USA* **96:** 6054–6059

Muskus MJ, Preuss F, Fan JY, Bjes ES, Price JL (2007) *Drosophila* DBT lacking protein kinase activity produces long-period and arrhythmic circadian behavioral and molecular rhythms. *Mol Cell Biol* **27:** 8049–8064

Nagoshi E, Saini C, Bauer C, Laroche T, Naef F, Schibler U (2004) Circadian gene expression in individual fibroblasts: cell-autonomous and self-sustained oscillators pass time to daughter cells. *Cell* **119:** 693–705

Nakajima M, Imai K, Ito H, Nishiwaki T, Murayama Y, Iwasaki H, Oyama T, Kondo T (2005) Reconstitution of circadian oscillation of cyanobacterial KaiC phosphorylation *in vitro*. *Science* **308:** 414–415

Nguyen VT, Giannoni F, Dubois MF, Seo SJ, Vigneron M, Kedinger C, Bensaude O (1996) *In vivo* degradation of RNA polymerase II largest subunit triggered by alpha-amanitin. *Nucleic Acids Res* **24:** 2924–2929

Oster H, Yasui A, van der Horst GT, Albrecht U (2002) Disruption of mCry2 restores circadian rhythmicity in mPer2 mutant mice. *Genes Dev* **16:** 2633–2638

Pando MP, Morse D, Cermakian N, Sassone-Corsi P (2002) Phenotypic rescue of a peripheral clock genetic defect via SCN hierarchical dominance. *Cell* **110:** 107–117

Pittendrigh CS (1954) On temperature independence in the clock system controlling emergence time in Drosophila. *PNAS* **40:** 1018–1029

Reinke H, Saini C, Fleury-Olela F, Dibner C, Benjamin IJ, Schibler U (2008) Differential display of DNA-binding proteins reveals heat-shock factor 1 as a circadian transcription factor. *Genes Dev* **22:** 331–345

Reppert SM (2006) A colorful model of the circadian clock. *Cell* **124:** 233–236

Ripperger JA, Schibler U (2006) Rhythmic CLOCK-BMAL1 binding to multiple E-box motifs drives circadian Dbp transcription and chromatin transitions. *Nat Genet* **38:** 369–374

Rougemont J, Naef F (2007) Dynamical signatures of cellular fluctuations and oscillator stability in peripheral circadian clocks. *Mol Syst Biol* **3:** 93

Schmidt EE, Schibler U (1995) Cell size regulation, a mechanism that controls cellular RNA accumulation: consequences on regulation of the ubiquitous transcription factors Oct1 and NF-Y and the liver-enriched transcription factor DBP. *J Cell Biol* **128:** 467–483

Smith EF (2002) Regulation of flagellar dynein by the axonemal central apparatus. *Cell Motil Cytoskeleton* **52:** 33–42

So WV, Rosbash M (1997) Post-transcriptional regulation contributes to *Drosophila* clock gene mRNA cycling. *EMBO J* **16:** 7146–7155

Takahashi JS (2004) Finding new clock components: past and future. *J Biol Rhythms* **19:** 339–347

Takeuchi T, Hinohara T, Kurosawa G, Uchida K (2007) A temperature-compensated model for circadian rhythms that can be entrained by temperature cycles. *J Theor Biol* **246:** 195–204

Taylor P, Hardin PE (2008) Rhythmic E-box binding by CLK–CYC controls daily cycles in per and tim transcription and chromatin modifications. *Mol Cell Biol* **28:** 4642–4652

Toh KL, Jones CR, He Y, Eide EJ, Hinz WA, Virshup DM, Ptacek LJ, Fu YH (2001) An hPer2 phosphorylation site mutation in familial advanced sleep phase syndrome. *Science* **291:** 1040–1043

Tomita J, Nakajima M, Kondo T, Iwasaki H (2005) No transcription–translation feedback in circadian rhythm of KaiC phosphorylation. *Science* **307:** 251–254

Tsuchiya Y, Akashi M, Nishida E (2003) Temperature compensation and temperature resetting of circadian rhythms in mammalian cultured fibroblasts. *Genes Cells* **8:** 713–720

Vanselow K, Vanselow JT, Westermark PO, Reischl S, Maier B, Korte T, Herrmann A, Herzel H, Schlosser A, Kramer A (2006) Differential effects of PER2 phosphorylation: molecular basis for the human familial advanced sleep phase syndrome (FASPS). *Genes Dev* **20:** 2660–2672

Xu Y, Padiath QS, Shapiro RE, Jones CR, Wu SC, Saigoh N, Saigoh K, Ptacek LJ, Fu YH (2005) Functional consequences of a CKIdelta mutation causing familial advanced sleep phase syndrome. *Nature* **434:** 640–644

Yoo SH, Yamazaki S, Lowrey PL, Shimomura K, Ko CH, Buhr ED, Siepka SM, Hong HK, Oh WJ, Yoo OJ, Menaker M, Takahashi JS (2004) PERIOD2::LUCIFERASE real-time reporting of circadian dynamics reveals persistent circadian oscillations in mouse peripheral tissues. *Proc Natl Acad Sci USA* **101:** 5339–5346

Zheng B, Albrecht U, Kaasik K, Sage M, Lu W, Vaishnav S, Li Q, Sun ZS, Eichele G, Bradley A, Lee CC (2001) Nonredundant roles of the mPer1 and mPer2 genes in the mammalian circadian clock. *Cell* **105:** 683–694

